

Post-perovskite memristive materials for hardware neural networks

Project duration: 2021-2022
Project manager: Prof. Dr hab. Konrad Szaciłowski
Academic Centre of Materials and Nanotechnology

ABSTRACT:

Memristors are unique electronic elements that are passive (they can dissipate energy and are not power sources) and have a state memory. In functional terms, they are similar to synapses present in animal nervous systems. These features mean that memristors are considered as the main building blocks of future computers. Their existence was theoretically predicted in the 1970s, which initiated very intensive research work. As part of this project, it was planned to develop a synthesis of new semiconductor materials that exhibit simultaneously the characteristics of ferroelectrics – materials that show the ordering of the internal structure under the influence of an external electric field. Materials that exhibit such characteristics include lead halide perovskites, photovoltaic materials successfully tested also in memristive applications. The main limitation of their widespread use is high sensitivity to moisture and their toxicity. In this project, it was planned to design and test two classes of chemical compounds, which on the one hand will combine semiconductor and ferroelectric features, and on the other hand are free from drawbacks of lead perovskites (higher durability and lower toxicity). In addition, it was anticipated that new materials would enable fine tuning of electrical properties to obtain memristors with the desired properties. These materials were accurately characterized in terms of structure and electrical properties. It was planned to make a series of thin film memristors, the operation of which was based on the modulation of the energy barrier at the metal-semiconductor junction (the so-called Schottky barrier). This configuration should provide much better parameters of the memristor, in particular greater durability and lower energy consumption in the switching process. It was anticipated that the combination of semiconductor and ferroelectric features in one material could bring many benefits from the point of view of the operation of the memristors: faster switching, longer state retention time, multi-state switching.

INTRODUCTION:

The constantly increasing demands for computational power stimulate continuous research on novel computational technologies. One of the limitations of classical computational technology is the so-called von Neumann bottleneck – the necessity of the constant information flow from the memory to the processor. Therefore, new memory technologies as well as in-memory computation approaches are explored. Memristors – fundamental electronic elements with memory features, are therefore considered as a Holy Grail of future computing. Current proposal addresses some material issues of memristors and is aimed at the quest for new phenomena that can potentially boost performance of memristors. The main aim of the project was to find a relation between ferroelectricity and memristive switching of Schottky junctions. It was achieved in several subsequent steps including: (i) the design and synthesis of new semiconducting materials with ferroelectric properties, their detailed studies, (ii) fabrication of memristors based on these materials, and (iii) verification of memristor performance is a series of neuromimetic computing tests. The working hypothesis assumed that the combination of memristive effects resulting from modulation of the Schottky barrier height combined with the rearrangement of electric dipoles due to ferroelectric ordering should result in better performance of the memristors in at least two of the following aspects: (i) increased information retention time, (ii) decreased energy consumption, (iii) higher ON/OFF current ratio, and (iv) increased nonlinearity of electrical characteristics.

As a cherry on top, a new effect resulting from resonant coupling of ferroelectric and memristive switching was searched for: this kind of coupling, never addressed neither experimentally nor theoretically, should lead to completely new switching patterns in memristors and a complex switching dynamics. Large efforts towards the observation of this novel effect was undertaken.

The realization of this ambitious and challenging research programme followed a path of several, partially overlapping research objectives.

(i) A series of both p and d block element complexes was designed and synthesized. These included bromo- and iodo-complexes of iron, copper, nickel, iron, bismuth, and antimony (also with additional polypyridine or quinolone ligands) and appropriate cations (quaternary ammonium cations, viologens and protonated amines with extended aromatic substituents). Preliminary results obtained for similar structures indicated the presence of interesting electrical properties of these materials. The selection of this family of compounds was justified for their prospective ferroelectricity – among several hundreds of ferroelectric coordination compounds halide complexes show the highest Curie-Weiss temperature. Furthermore, the presence of heavy halide ligands usually stabilises the structure and increases electrical conductivity due to the formation of halide bonds, the presence of aromatic moieties shows similar effects due to stacking interactions.

(ii) Stable and well-characterized complexes were used for the fabrication of thin layer ferroelectric Schottky junction memristors and their properties were characterized in detail. The special attention was paid to the conductivity switching resulting from modulation of the Schottky barrier height coupled with dipolar polarization of ferroelectric materials. Electronic structure of junctions, switching dynamics and interplay between molecular structure, spectroscopic properties and memristive properties were explored. Here, the predicted resonant switching could be observed as a consequence of the effects of material polarization on the structure and properties of Schottky junctions.

(iii) The performance of memristors was evaluated in a series of neuromimetic experiments, in which electrical nonlinearity and synaptic properties (plasticity-related memory effects) were explored in the context of signal analysis and information processing.

As a final result, the project should yield a library of new, fully characterized coordination compounds with semiconducting, ferroelectric, and memristive properties, description of new physical phenomenon of resonant memristive switching, and a further development of neuromimetic information processing elements.

SUMMARY OF RESULTS:

The effect of morphology and composition on optical and electrical characteristics of a series of pyridinium-based bismuth iodide complexes were investigated. Pyridine (py), 4-aminopyridine (4-Ampy), 4-methylpyridine (4-Mepy), 4-dimethylaminopyridine (4-Dmepy), and 4-pyridinecarbonitrile (4-CNpy) were selected as organic substrates with various functional groups at the para position with different electron-donating and electron withdrawing strengths. The crystallography data represent different bismuth iodide fragments in the resulting structures, a 1D chain of [BiI₄]ⁿ⁻ in the 4-AmpyBiI₃ derivative was observed. However, in 4-MepyBiI₃ and 4-DmepyBiI₃, 4-CNpyBiI₃ salts, we could detect discrete 0D motifs such as [Bi₂X₉]³⁻, [Bi₂X₁₀]⁴⁻, and [Bi₄I₁₆]⁴⁻, respectively. Diffraction reflectance spectroscopy (DRS) was used to conduct an experimental investigation into the nature of the band gap of these materials, and the results are in good agreement with values based on density functional theory (DFT) calculations. Structural investigation inferred that the crystal packing is mainly stabilised by N-H...I and comparatively weak I...I bonding between the cation and anion and further stabilized by weak I...π and I-π interactions. The Hirshfeld surface (HS) analysis was employed to explore the non-covalent intermolecular interactions between bismuth iodide fragments and pyridinium cations that are quantitatively responsible for crystal packing in the solid-state. The void analysis by Crystal explorer shows that voids occupied less of the unit cell volume and in case of, and in case of the 4-AmpyBiI₃ derivative which crystals grow in 1D morphology, it shows the lowest value of void percentage (4.3%). Spectroscopic investigations reveal details of electronic interactions within the lattice, highlighting the role of electron donor and electron acceptor substituents in pyridinium cations and subtle differences in hybridization between bismuth and iodide centres. The thermogravimetry-differential thermal analysis (TG-DTA) measurements show that the functionalization of pyridinium cation in the mentioned crystalline structures lead to the of structures up to 250°C. The linear sweep voltammetry (LSV) technique was applied to measure current-voltage scans (IV) of the devices made of thin layers of synthetic materials on ITO/glasses with copper as top electrode, in the temperature range between 243.15 to 453.15 K, and it indicates significant conductivity of the samples at the level of 10-20 mS/pixel at 298.15 K: the highest one was recorded for 4-CNpyBiI₃, and the lowest for 4-AmpyBiI₃. Spectroscopic ellipsometry was applied for measuring thickness of thin layers (ranges between 150 to 200 nm), refractive index (n) more than 2 at 632 nm (1.96 eV), and dielectric constant of layers ranges from 4 to 6 in the ranges (320 nm to 632 nm), except for 4-CNpyBiI₃ with lower values. X-ray absorption spectroscopy (XAS) at the Bi L₃-edge shows that the positions of the white line in all derivatives are very close values and changes from 13419.2 eV for 4-AmpyBiI₃ to 13422.0 eV for 4-DmepyBiI₃, which resulted from similar oxidation state and the electronic environment of bismuth centers surrounded by iodide ions.

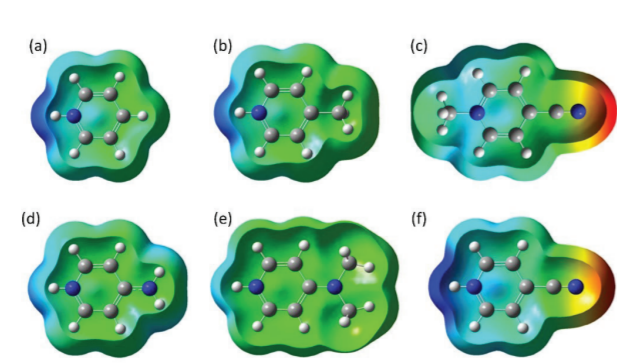


Figure 1. Converged molecular geometries of the studied cations and electrostatic potential distribution mapped onto electron density isosurfaces.

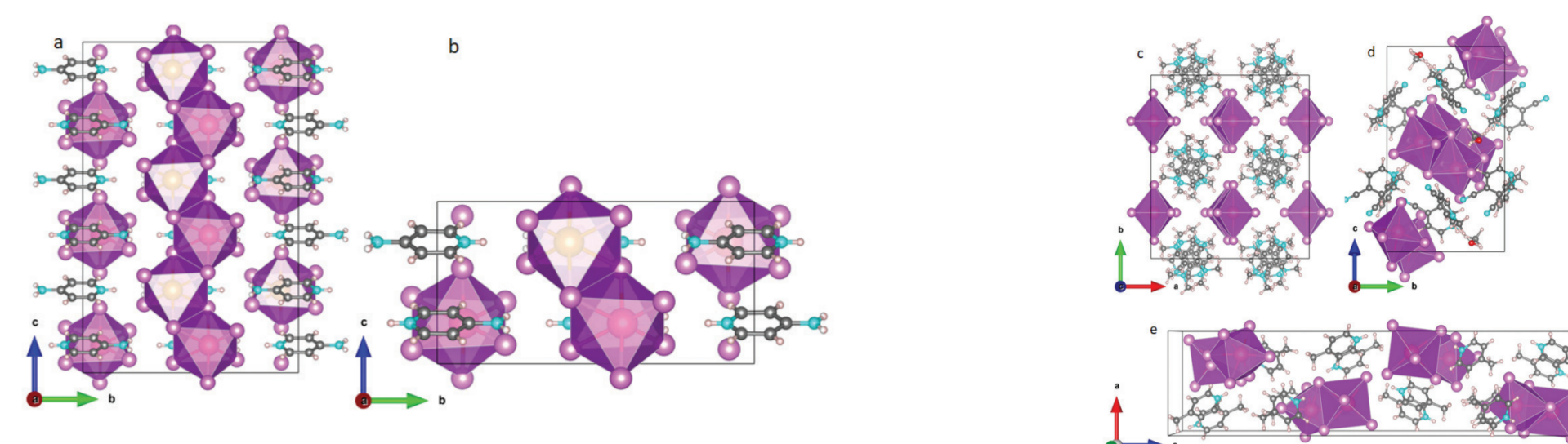


Figure 2. (a) 4-AmpyBiI₃ side view of 1D growth of bismuth iodide fragments in crystalline structures. Perspective view of unit cell by edge sharing of (b) infinite BiI₆ octahedra in 4-AmpyBiI₃; (c) two BiI₆ octahedra in 4-DmepyBiI₃ (d) four BiI₆ octahedra in 4-CNpyBiI₃; (e) by face-sharing of two BiI₆ octahedra in 4-MepyBiI₃.

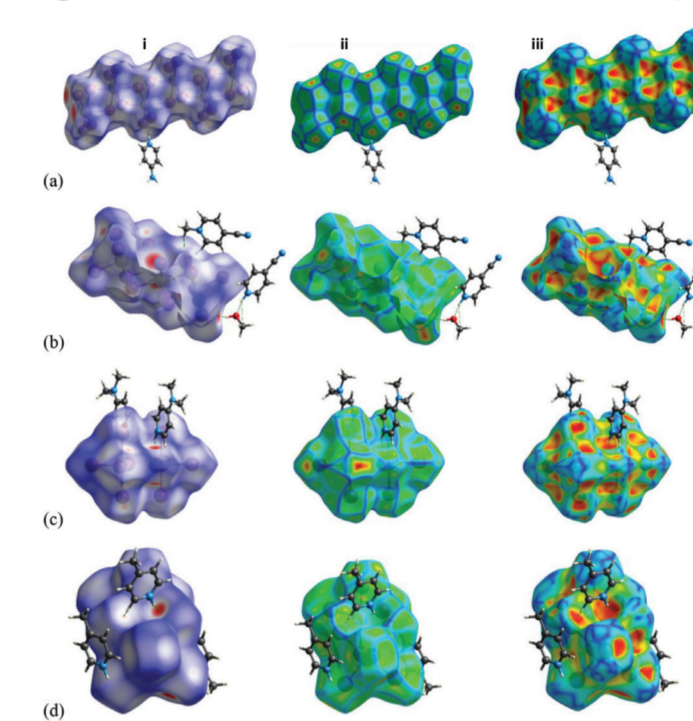


Figure 3. (i) 3D dnrm surface of (a) 4-AmpyBiI₃ in the range -0.4527 to 1.1099, (b) 4-MepyBiI₃ ranging from -0.3428 to 1.2451 (c) 4-DmepyBiI₃ in the range -0.3012 to 1.1518, (d) 4-CNpyBiI₃ in the range of -0.3383 a.u. (red) to 1.3823 a.u. (blue), (ii) curvedness in the range of (-4.0000 to 0.4000), (iii) shape index in the range of (-1.0000 to 1.0000).

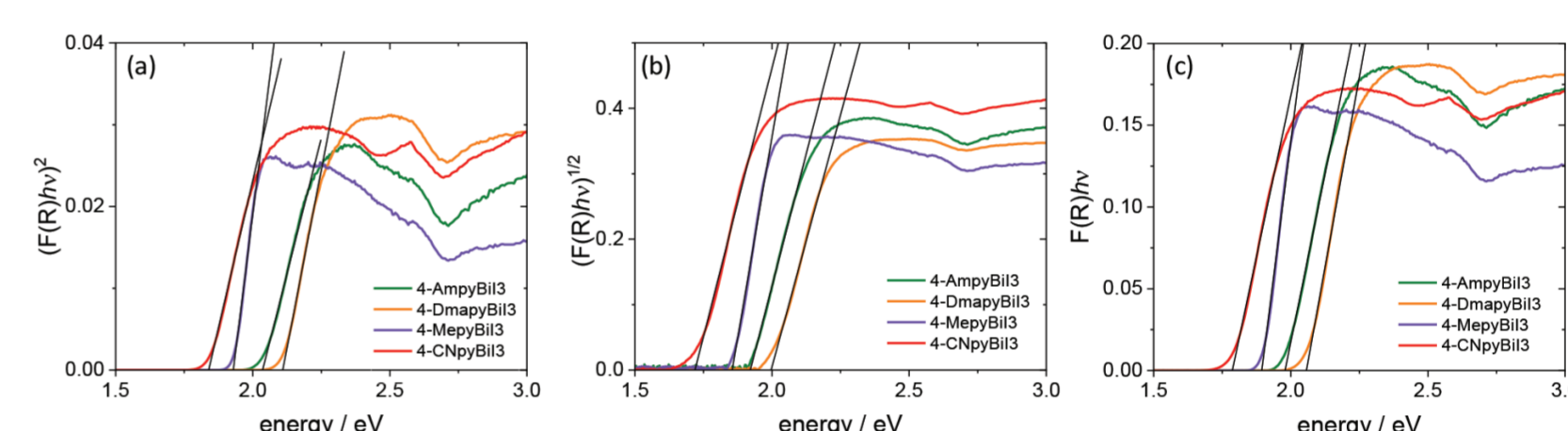


Figure 4. UV-vis diffuse reflectance spectra (Tauc plots derived from Kubelka-Munk function) for a direct (a) and an indirect (b) transitions as well as calculated for molecular semiconductors (c).

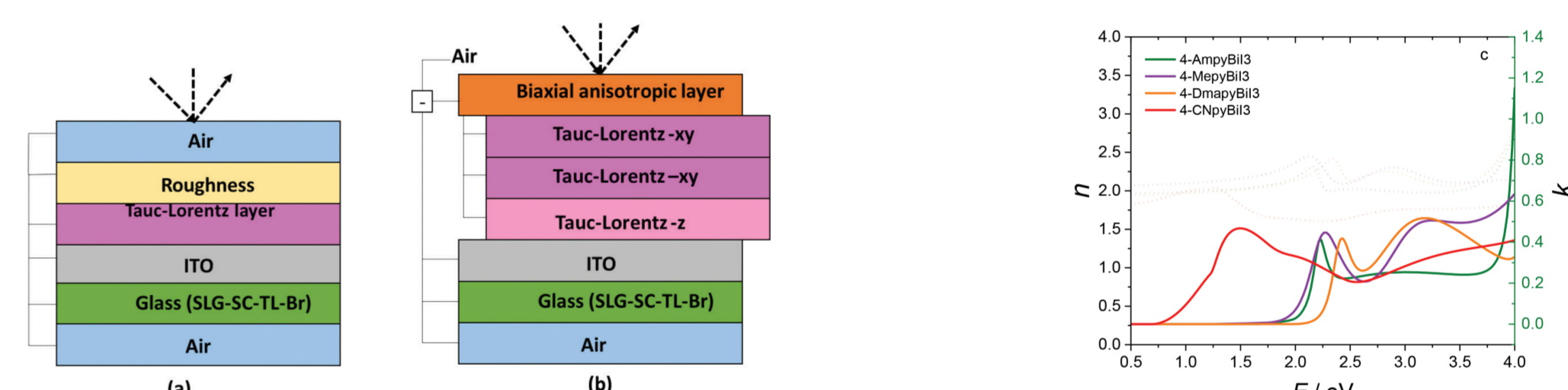


Figure 5. Schematic representation of the models used for fitting experimental data from spectroscopic ellipsometry for (a) 4-MepyBiI₃ or 4-DmepyBiI₃, or 4-AmpyBiI₃, (b) biaxial anisotropic model for 4-CNpyBiI₃ as Tauc-Lorentz layers. (c) Real (dotted) and imaginary (solid) parts of a complex dielectric function of the layers. Thickness of the glass substrate was fixed at 1100000 nm.

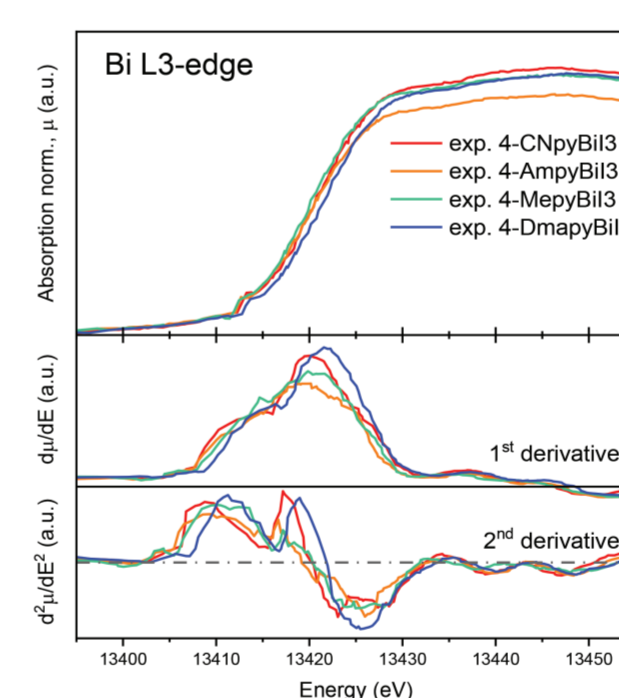


Figure 6. Experimental XAS spectra for 4-CNpyBiI₃, 4-AmpyBiI₃, 4-MepyBiI₃ and 4-DmepyBiI₃ complexes at the L₃ edge are presented on top, together with their first (middle) and 2nd (bottom) derivatives. The dotted grey line stands on the 2nd derivative plot and stands for 0. The derivatives were additionally smoothed using a Savitzky-Golay filter.

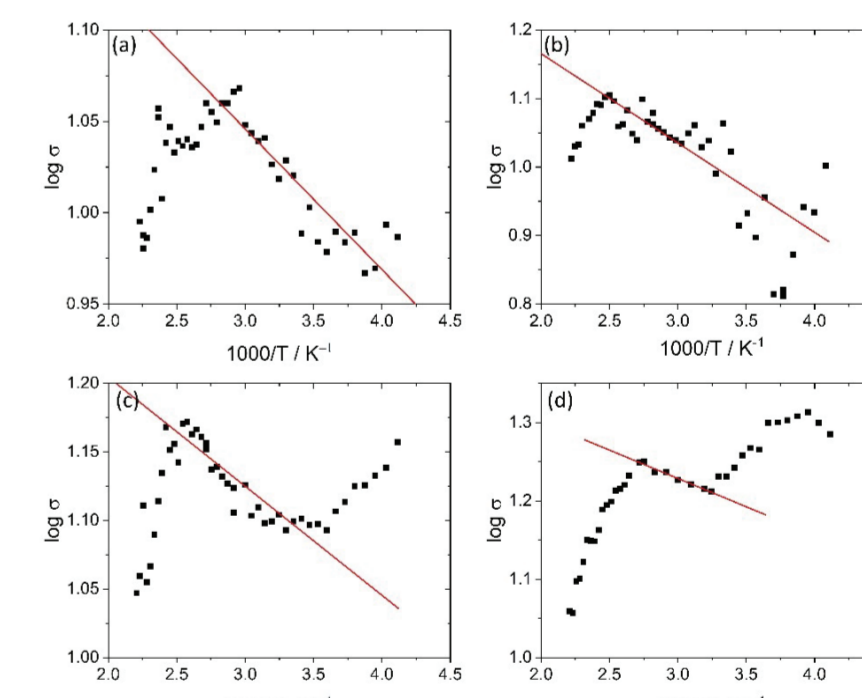


Figure 7. Arrhenius plots for electrical conductivity of 4-AmpyBiI₃ (a), 4-DmepyBiI₃ (b), 4-MepyBiI₃ (c) and 4-CNpyBiI₃ (d). Red line is a linear fit to the Arrhenius equation.

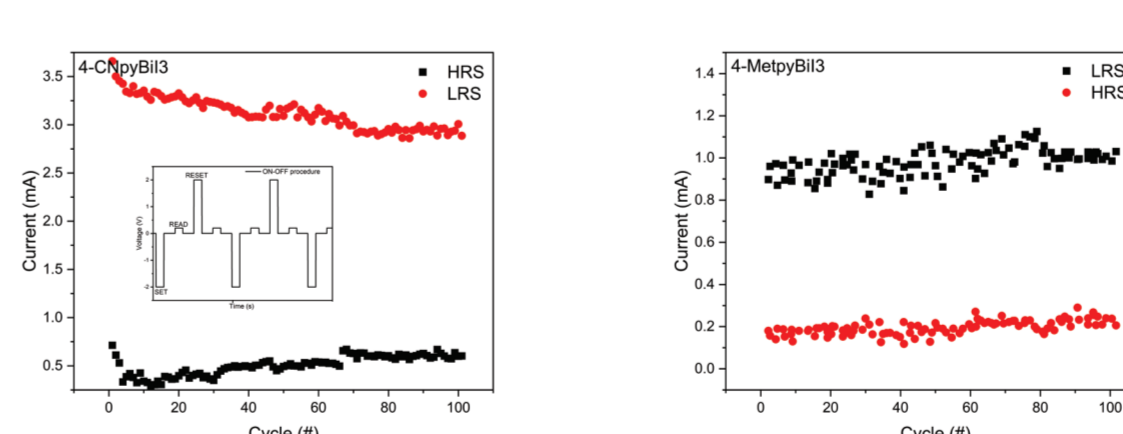


Figure 8. On-off ratios of the devices made of 4-CNpyBiI₃ and 4-MepyBiI₃, the range of ±2 V was chosen as the set and rest voltage and the read point was +0.2 Mv. The width of all pulse was 0.1 s.

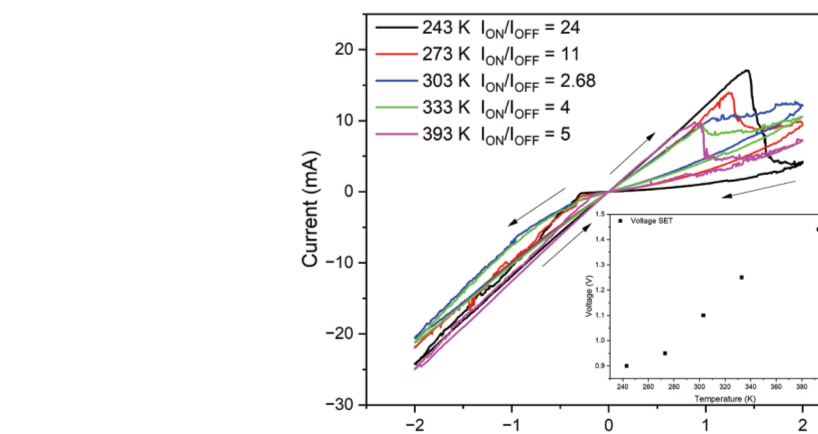


Figure 9. I-V plots recorded for 4-CNpyBiI₃ under different temperatures. Inset depicted the maximum current point dependence in RESET process to temperature changes.

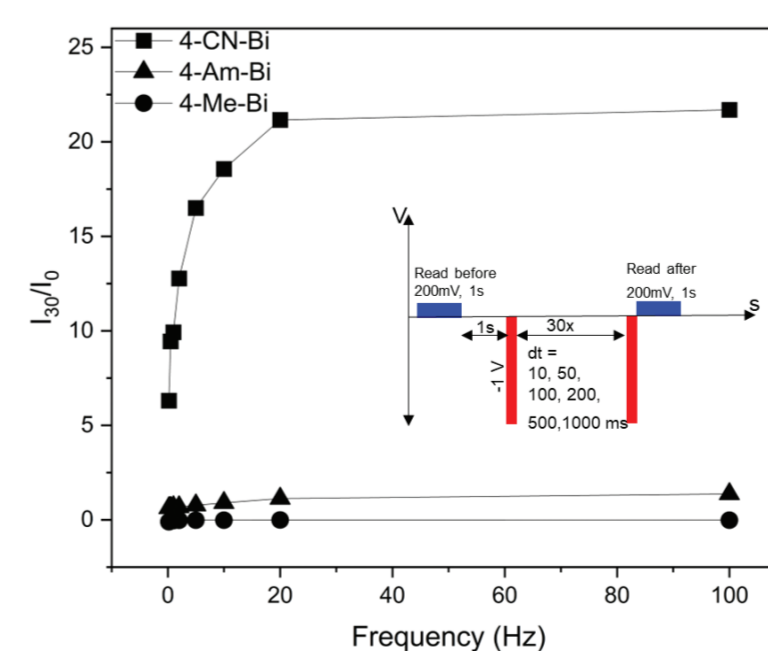


Figure 10. Frequency-dependent EPSC of 4-CNpyBiI₃, 4-MepyBiI₃, 4-AmpyBiI₃. Inset represent the applied procedure.

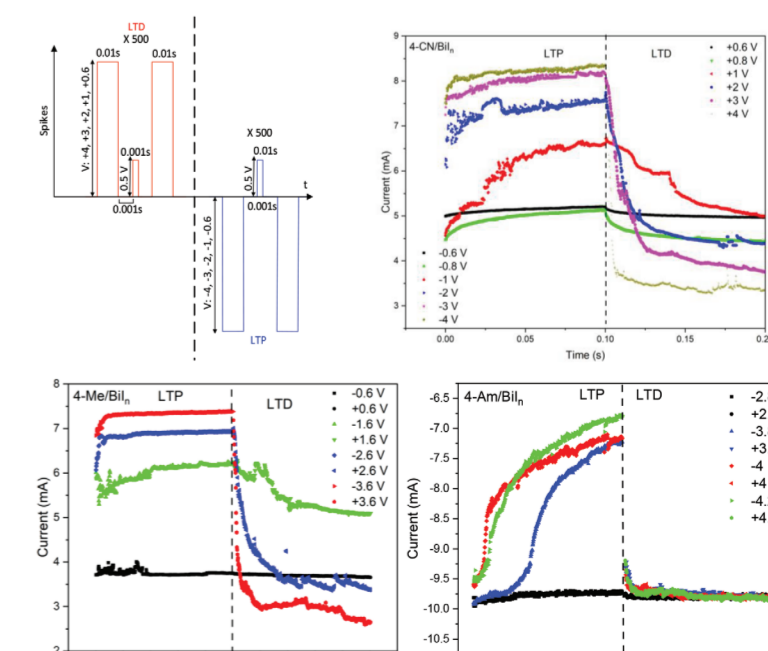


Figure 11. LTP and LTD experiments on 4-CNpyBiI₃, 4-MepyBiI₃, 4-AmpyBiI₃.

